HAL open science

A dynamic subgraph-capacity model for multiple shortest paths and application to CO2/contrail-safe aircraft trajectories

Céline Demouge, Marcel Mongeau, Nicolas Couellan, Daniel Delahaye

To cite this version:

Céline Demouge, Marcel Mongeau, Nicolas Couellan, Daniel Delahaye. A dynamic subgraph-capacity model for multiple shortest paths and application to CO2/contrail-safe aircraft trajectories. 2022. hal-03900872v1

HAL Id: hal-03900872

https://enac.hal.science/hal-03900872v1

Preprint submitted on 15 Dec 2022 (v1), last revised 6 Jun 2023 (v2)

HAL is a multi-disciplinary open access archive for the deposit and dissemination of scientific research documents, whether they are published or not. The documents may come from teaching and research institutions in France or abroad, or from public or private research centers.

L'archive ouverte pluridisciplinaire **HAL**, est destinée au dépôt et à la diffusion de documents scientifiques de niveau recherche, publiés ou non, émanant des établissements d'enseignement et de recherche français ou étrangers, des laboratoires publics ou privés.

A dynamic subgraph-capacity model for multiple shortest paths and application to CO_2/contrail-safe aircraft trajectories

Céline Demouge[a,*], Marcel Mongeau[a], Nicolas Couellan[a,b], Daniel Delahaye[a]

[a]*ENAC, Université de Toulouse, 7 avenue Edouard Belin, Toulouse, 31400, France*
[b]*Institut de Mathématiques de Toulouse, UMR 5219, Université de Toulouse, CNRS, UPS, Toulouse Cedex 9, 31062, France*

Abstract

Finding a shortest path with various constraints and cost functions is a common problem in operations research. This paper deals with the special case of the problem of computing multiple shortest paths with capacity constraints on a subgraph that evolves over time. Multiple shortest paths is understood as paths for each vehicle considered. The static special case is modeled as a *Mixed Integer Linear Programming* (MILP) problem, so that it can be solved directly by a standard commercial solver. The time-dependent nature of the problem is then modeled thanks to a sliding-window approach. This study is motivated by the problem of minimizing the environmental impact of air transport at the level of a complete air network, considering thereby several aircraft. Both CO_2 and non-CO_2 effects are taken into account to calculate the impact. The proposed methodology takes into account a network point of view where airspace (subgraph) capacities evolve as well as the traffic itself over time. Encouraging numerical results on the CO_2/contrail-safe aircraft trajectories application are obtained and show that the environmental impact can be reduced while maintaining safety by guaranteeing the respect of airspace capacities.

Keywords: Subgraph constrained time-dependent shortest path problem,

*Corresponding author

Email addresses: celine.demouge@enac.fr (Céline Demouge), mongeau@recherche.enac.fr (Marcel Mongeau), nicolas.couellan@recherche.enac.fr (Nicolas Couellan), delahaye@recherche.enac.fr (Daniel Delahaye)

December 15, 2022

1. Introduction

Finding a shortest path is a common problem in operations research. The literature presents various way to solve such problems. The graph version of the problem can be addressed by integer linear programming [1], or other efficient algorithms such as Dijkstra's algorithm [2], A* [3] or Bellman's algorithm [4] which is based on dynamic programming. In some cases, optimal control techniques [5] can be used, especially if the path is to be computed in a continuous space and not on a graph. The constrained variant of the shortest path problem is subject to constraints that typically involves an upper limit on a function of arcs. For instance, the goal can be to minimize the distance traveled by a vehicle with an upper bound on the travel time. This type of problem is usually expressed for one vehicle, for one path. It is an NP-hard problem for which some efficient methods have been developed [6, 7, 8].

Some other problems compute several shortest paths, *i.e.*, several vehicles are considered via a global criterion to be minimized. This is the case for the *traffic assignment problem* (TAP) which aims at reaching an equilibrium for the vehicles or for the whole system. The type of chosen equilibrium determines the objective function to be minimized. An example is the *Wardrop user and system equilibrium* [9, 10]. The problem is subject to flow conservation constraints and capacity constraints on arcs and, in the case of *system equilibrium*, minimizes the average journey cost. This problem considers cooperation and possibly a decentralized management of the traffic. On the other hand, the *user equilibrium* is reached when no vehicle can lower its transportation cost through unilateral action. It is for instance used for road network application, where roads do not have infinite capacity but the number of vehicles that can use each road in a given amount of time is limited.

The previously mentioned problems take into account the arcs of the graph to define routes, and possibly capacities on these routes. However, there are also other types of problems in which the grain is coarser: nodes are defined by geographical sector, and a total capacity on each of these sectors is imposed. This special case therefore involves capacities on the *vertices* of the graph. This type of problem appears in air transportation: it is then named *air traffic flow management problem* (ATFMP), originally

defined in [11]. The objective function of the ATFMP is the total cost of aircraft delays, but variants can be derived by considering other objective functions. For example, the total cost of trajectories in terms of flight time, distance flown or CO_2 emitted can be taken into account. Optimization models addressing this problem typically involves the following decisions to be made for each flight:

- which sector to fly and when (which may induce speed modulations)?
- when to take off (by inflicting delays with respect to the scheduled departure time)?

Various capacity upper bounds are imposed on:

- the total number of aircraft in each sector at any given time (sector capacity constraints),
- the total number of aircraft in each airport at any given time (airport capacity constraints).

This is a large-grained problem, but it is also necessary to take into account the more precise spatial scale of the arcs to know where to fly through a sector at a given time. This is done in the variant of the ATFM problem that involves rerouting (ATFMRP), and is solved in [12] (in its deterministic version). This problem is very detailed since it completely defines the trajectory followed, and it decides the speed of each aircraft on flown arcs. It takes into account a cost on each arc. This cost can be the flight time, the distance flown, or estimated CO_2 emissions on this arc, for each aircraft.

This paper presents a model of multiple shortest paths problem with capacity constraints on subgraphs. The main difference with previous works is that the capacity constraints are not defined on vertices (that can represent sectors) but on subsets of arcs. A particular application of this problem is discussed: the minimization of the global impact of air traffic on an area taking into account CO_2 and contrails.

The contributions of this study could be summarized and listed as:

- an optimization model in the static case that:
  - computes simultaneously (not sequentially) a path for each vehicle considered,

  - takes into account capacity constraints on subgraphs;

- an optimization model for the dynamic extension with time-dependent costs and constraints;

- a low environmental-impact aircraft trajectory application with:

  - a network approach for contrail mitigation,
  - a realistic illustrative instance made publically available,
  - preliminary numerical experiments that show that contrails can be mitigated at the network scale.

This paper presents first, in Section 2, an optimization model for the static case and its extension to the time-dependent problem. The application to the contrail-avoidance aircraft trajectory problem is studied in Section 3. Promising numerical experiments are shown and discussed in Section 4 through a sensitivity analysis of the different parameters involved. Section 5 presents general conclusions and perspectives. Appendix A gives the time-discretized optimization model, and Appendix B details how the application input data are computed.

2. Mathematical optimization model

This section presents the mathematical optimization models for the subgraph-capacity multiple shortest path problem: Subsection 2.1 presents the static case while Subsection 2.2 addresses the time-dependent case.

2.1. Static case

This subsection focuses on the subgraph-capacity multiple shortest path problem in the static case (input data do not evolve with time).

The classical shortest-path problem on a graph involves only one vehicle and is modelled as follows. Let $G = (V, A)$ be a directed weighted graph, where V is the set of vertices, A is the set of arcs, and $w : A \to \mathbb{R}$ is the weight function. Let $s \in V$ be the start of the path, and $e \in V$ be the end of the path. Considering that the decision-variable vector X has a component $x_{u,v}$ for each arc $(u, v) \in A$, where $x_{u,v}$ indicates whether the arc (u, v) is part of the solution path or not, the optimization formulation of the shortest-path problem is:

$$\min_{X} \quad \sum_{(u,v)\in A} w_{u,v} x_{u,v} \tag{1a}$$

$$\text{s.t.} \quad \sum_{(u,v)\in A} x_{u,v} - \sum_{(v,u)\in A} x_{v,u} = 0,\ u \in V\backslash\{s,e\} \tag{1b}$$

$$\sum_{(s,v)\in A} x_{s,v} - \sum_{(v,s)\in A} x_{v,s} = 1 \tag{1c}$$

$$\sum_{(e,v)\in A} x_{e,v} - \sum_{(v,e)\in A} x_{v,e} = -1 \tag{1d}$$

$$X \in \{0,1\}^{|A|}, \tag{1e}$$

where (1b), (1c) and (1c) are the classical network flow conservation constraints (see for instance [1]) that ensure that the solution is a path from s to e (the incoming flow is equal to the outcoming flow on each vertex other than the source and the end).

This model can be adapted in the case of several vehicles with vehicle-specific weight functions, whose (u,v)-components are noted $w_{u,v,i},\ (u,v) \in A,\ i = 1,2,\ldots,M$, where M is the number of vehicles, and for each vehicle $i = 1,2,\ldots,M$, a start vertex $s_i \in V$, and an end vertex $e_i \in V$. Defining a decision-variable vector X_i for each vehicle, $i = 1,2,\ldots,M$, the optimization model for the multiple shortest-path problem then reads:

$$\min_{X_1,\ldots,X_M} \quad \sum_{i=1}^{M} \sum_{(u,v)\in A} w_{u,v,i} x_{u,v,i} \tag{2a}$$

$$\text{s.t.} \quad \sum_{(u,v)\in A} x_{u,v,i} - \sum_{(v,u)\in A} x_{v,u,i} = 0,\ u \in V\backslash\{s_i,e_i\},\ i = 1,2,\ldots,M \tag{2b}$$

$$\sum_{(s,v)\in A} x_{s_i,v,i} - \sum_{(v,s_i)\in A} x_{v,s_i,i} = 1,\ i = 1,2,\ldots,M \tag{2c}$$

$$\sum_{(t,v)\in A} x_{e_i,v,i} - \sum_{(v,e_i)\in A} x_{v,e_i,i} = -1,\ i = 1,2,\ldots,M \tag{2d}$$

$$X_i \in \{0,1\}^{|A|},\ i = 1,2,\ldots,M. \tag{2e}$$

Finally, a subgraph-capacity extension can be defined, provided a partition $\bigcup_{k=0}^{N} A_k = A$ of the set of arcs is given with corresponding capacities

$C_k,\ k = 1, 2, \ldots, N$. In the sequel, we shall call *sector* each of the subsets $A_k,\ k = 1, 2, \ldots, N$.

Finally, we define an auxiliary decision-variable vector, Y_i, for each vehicle i, $i = 1, 2, \ldots, M$, whose k^{th} component, $y_{k,i}$, indicates whether vehicle i uses arcs of sector $A_k,\ k = 1, 2, \ldots, N$. The optimization model for the subgraph-capacity multiple shortest-path problem is:

$$\min_{X,Y} \quad \sum_{i=1}^{M} \sum_{(u,v)\in A} w_{u,v,i} x_{u,v,i} \tag{3a}$$

$$\text{s.t.} \quad \sum_{(u,v)\in A} x_{u,v,i} - \sum_{(v,u)\in A} x_{v,u,i} = 0,\ u \in V \backslash \{s_i, e_i\},\ i = 1, 2, \ldots, M \tag{3b}$$

$$\sum_{(s,v)\in A} x_{s_i,v,i} - \sum_{(v,s_i)\in A} x_{v,s_i,i} = 1,\ i = 1, 2, \ldots, M \tag{3c}$$

$$\sum_{(t,v)\in A} x_{e_i,v,i} - \sum_{(v,e_i)\in A} x_{v,e_i,i} = -1,\ i = 1, 2, \ldots, M \tag{3d}$$

$$\sum_{i=1}^{M} y_{k,i} \leq C_k,\ k = 1, 2, \ldots, N \tag{3e}$$

$$y_{k,i} = 1 \text{ iff } \sum_{(u,v)\in A_k} x_{u,v,i} \geq 1,\ i = 1, 2, \ldots, M,\ k = 1, 2, \ldots, N \tag{3f}$$

$$X_i \in \{0, 1\}^{|A|},\ i = 1, 2, \ldots, M \tag{3g}$$

$$Y_i \in \{0, 1\}^{N},\ i = 1, 2, \ldots, M. \tag{3h}$$

Constraints (3b), (3c) and (3d) are the usual path flow conservation constraints for each vehicle, and constraints (3e) and (3f) are the subgraph capacity constraints.

Constraints (3f) enforce the definition of the auxiliary binary variables $Y_1, Y_2, \ldots, Y_N$. These constraints can be linearized thanks to linearization techniques and can be written as continuous variables.

Proposition 1. *Each of the constraints (3f), $i = 1, 2, \ldots, M$, can be replaced*

and linearized by:

$$y_{k,i} \geq x_{u,v,i}, \ (u,v) \in A_k \tag{4}$$

$$y_{k,i} \leq \sum_{(u,v)\in A_k} x_{u,v,i} \tag{5}$$

$$y_{k,i} \in [0,1] \tag{6}$$

Proof. Consider a sector k and a vehicle i. Let $z_{k,i} = 1 - y_{k,i}$. Then, $z_{k,i} = \prod_{(u,v)\in A_k}(1 - x_{u,v,i})$. Thanks to classical reformulation techniques (see for instance [13]) on the product variable $z_{k,i}$, the desired result is obtained. □

2.2. Time-dependent case

This subsection defines the mathematical formulation of the problem in the case where input data evolve with time. In the general case, we are considering time-dependent costs. Moreover, constraints (3e) and (3f) can also be time-dependent in case where a sector is only occupied by the vehicle during a certain amount of time and it is not occupied when the vehicle is not in the sector yet/anymore. The associated time-discretized model can be found in Appendix A.

To take into account the release of the capacity of sectors by vehicles as they move, the paths are optimized for a succession of *(sliding) time windows*. More precisely, the paths on the graph are computed based on sector occupancy during the time interval. Then, the time is incremented by the sliding-window size Δt, and the start vertex s_i of each vehicle i is updated: it is replaced by the vertex reached by vehicle i in the previous sliding-window optimization. This process is illustrated by Figure 1. When, at the end of a time window, a vehicle is on an arc but not at a node, an artificial node is created. The process is stopped when each vehicle has reached its destination vertex $e_i, i = 1, 2, \ldots, M$. The entry time in the simulation of each vehicle is not artificially changed to coincide with the beginning of a time window. This time-window approach may lead to suboptimal solutions but is used as a resolution heuristic for the following reasons. First, the time-dependent shortest path for a single vehicle is already a difficult problem [14], not to mention the case involving several vehicles and capacity constraints. It would have been even more difficult for several vehicles with capacity constraints. Moreover, the time-window methodology is tailored to operational concerns. Indeed, all relevant information is not always known for the next time periods, and this time-sequential approach breaks the uncertainties at each time window, by taking into account updated information.

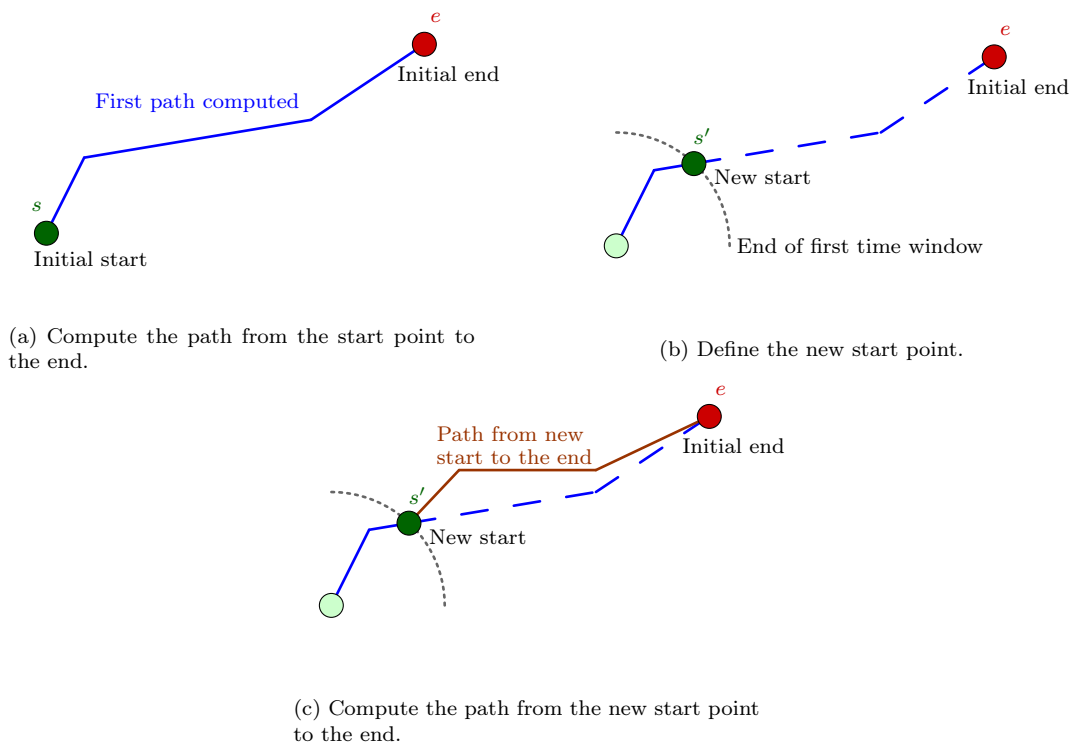

(a) Compute the path from the start point to the end.

(b) Define the new start point.

(c) Compute the path from the new start point to the end.

Figure 1: Sliding window computation of path. The final path is computed sequentially, in pieces, for each of the time windows.

The paths on the graph are computed taking into account the capacity constraints only for a duration corresponding to K times the length of the sliding window, as shown by Figure 2. More precisely, constraints (3f) are modified as follows:

$$y_{k,i} = 1 \text{ iff } \sum_{(u,v)\in A_{k,K\Delta t}} x_{u,v,i} \geq 1,\ i = 1, 2, \ldots, M,\ k = 1, 2, \ldots, N \tag{7}$$

where $A_{k,K\Delta t}$ is the subset of arcs from A_k that have at least one end accessible by vehicle i within a time less than $K\Delta t$ from s_i, where K is user-defined parameter.

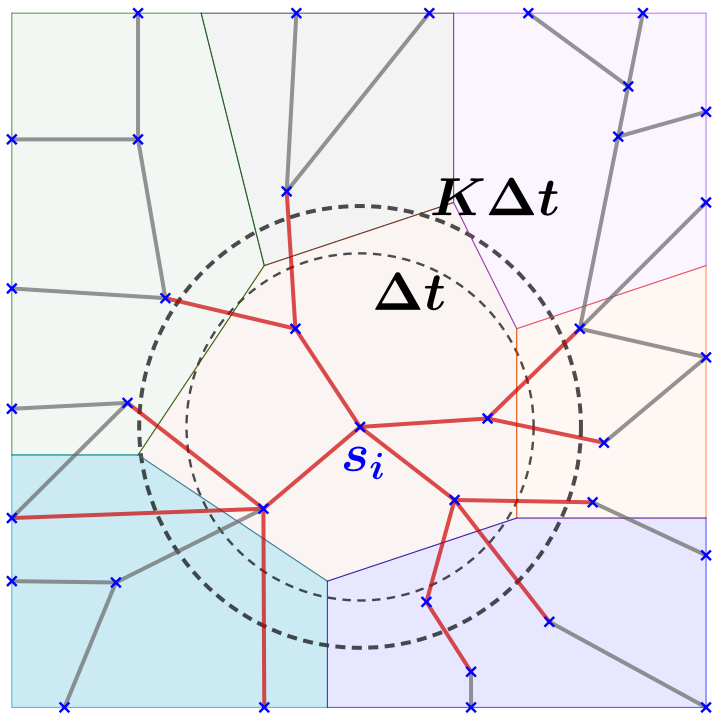

Figure 2: Capacity computation along time windows. We consider that a vehicle i consumes capacity of the sectors that are accessible from the start point s_i within a time less than $K\,\Delta t$ (here: capacity is consumed only on red arcs).

3. Application to contrail avoidance and CO_2 minimization

Air transport offers a study case with some particular features. First, it is possible to optimize on a global scale by acting on all the aircraft. Indeed, even if the planes are independent of each other, since they are owned by different airlines, the planned paths are controlled by an independent entity, named here the air traffic control. As mentioned earlier, the capacity of the air sectors must be considered, and cannot be exceeded for safety reasons. Finally, if the goal is to minimize the environmental impact of the aircraft flying through an area (a country or a set of countries for instance), then another particularity of air transportation has to be taken into account. Indeed, the environmental impact of air transport is not only due to CO_2 but also to non-CO_2 effects such as contrails. These non-CO_2 effects are still not perfectly understood scientifically, but it is certain that contrails have a

warming effect which is estimated at two thirds of the total radiative forcing due to aviation [3], as illustrated by Figure 3. It is therefore important to take these effects into account in the optimization.

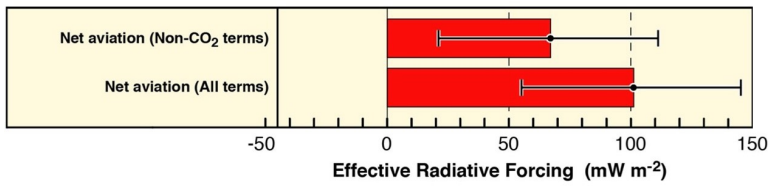

Figure 3: Comparison between CO_2 et non-CO_2 effects in aviation, adapted from [3]. It presents the effective radiative forcing estimated for non-CO_2 effects and total effects due to aviation (red) and the uncertainty (black) on these estimations.

This section first presents, in Subsection 3.1 the problem of contrails mitigation in air transport, and previous works on this issue. Subsection 3.2 then shows that contrail mitigation for several aircraft can be seen as an instance of the time-dependent subgraph-capacity multiple shortest path problem modeled in Section 2. Then, the cost function computation is detailed in Subsection 3.3. Finally, Subsection 3.4 gives more explanations about the required input data.

3.1. Air transportation and contrails mitigation

In recent years, driven by various initiatives, the issue of green aviation has become more prominent in the literature. Among these issues, non-CO_2 effects are a particularly important topic. Several methods taking different points of view and with different resolution strategies have been developed.

To solve the problem in the most general case, optimal control methods have been implemented. Since the constraints related to the mechanics of flight are enforced, the computed trajectory is flyable in the free space. The methods chosen differ according to the dimension of the instance addressed, the objective function considered, and the number of aircraft involved. Sridhar *et al.* [15] solve the problem in 2D thanks to optimal control by minimizing an objective function that takes into account contrail avoidance, fuel and flight time. It has been used on one-aircraft instances but also for trajectories between 12 city pairs. Hartjes *et al.* [16] solve the problem in 3D for a single aircraft also by minimizing fuel, time and time in contrails areas. Some other papers present methods taking into account time, such as [17].

Other studies rely on metaheuristics to solve the problem. For instance, Yin *et al.* [18] use genetic algorithms to compute transatlantic flight trajectory to mitigate the impact of contrails. Methods based on graphs are also used, like A* in [19].

Finally, other methodologies rely on MILP [20] or *mixed integer quadratic programming* (MIQP) [21] formulations.

Simorgh *et al.* remark in [22] that Air Traffic Management (ATM) considerations are generally not taken into account when multiple aircraft are considered, although the impact on airspace capacity and controller workload is certain. Indeed, a risk is to empty the spaces favorable to contrails by strongly congesting adjacent airspaces. Avoiding such situations is one of the main contributions of this paper.

3.2. General description of the application

In the sequel, the French upper airspace will be considered. Aircraft fly above France following a sequence of 3D or 2D points linked by straight-line segment routes. These points are named *waypoints* and all the waypoints, defined above France are the vertices of the graph. The segment routes defined between the waypoints define the set of arcs of the graph. The graph is thereby a directed graph, since aircraft routes can have a direction. The problem of finding a trajectory for a flight can therefore be likened to finding a path on a graph. The aim here is to minimize the global impact of all flights on the environment. More precisely, the goal is to minimize the total environmental cost while ensuring that the airspace capacities are not exceeded. The controller point of view is taken into account, and fairness among aircraft and airlines must be kept in mind. For this reason and in order not to find suboptimal solutions, a sequential (one aircraft at a time), greedy-like, computation of trajectories cannot be used, even though there are very efficient algorithms to solve shortest-path problems.

The application we consider in this study is solved only in the 2D plane, *i.e.*, the altitude is not to be decided by the optimizer. This choice is motivated by several operational reasons. First, the problem is designed to compute *cruise* trajectories (departing and arriving an airport is subject to numerous extra operational constraints), and the altitude is little modified in this phase. Moreover, the air traffic control does not know the weight of the plane, and therefore does not know if it is possible for the aircraft to climb. Thirdly, pilots usually choose the highest possible altitudes in order

to consume as little fuel as possible, and therefore we can assume that CO_2 is minimized by such a choice of altitude.

In the case of ground transportation, applications involving for instance cars on a road network, one can set a limited capacity per arc. In our air transportation application, the capacity limit is on areas (subsets of arcs), called *sectors*. These sectors represent subdivisions of the upper airspace, and more precisely a partition of the set of arcs. If the trajectories were to be computed sequentially, then some vehicles, the first ones, would be favored over the others. However, in the case of air transport, from the point of view of air traffic control, no airline should be favored over another, so such a sequential approach is not satisfactory. Above all, on the simple point of view of optimization, the greedy-like sequential approach is likely to lead to undesirable, suboptimal solutions.

The sliding-window approach mentioned before is adapted to the case of airspace capacity constraints, since that the capacities can be adapted in real time to the expected traffic. Moreover, operational capacity constraints are defined on time periods corresponding to the size of sliding windows.

3.3. Cost computation

As explained before, the goal here is to take into account CO_2 and non-CO_2 effects, and our application focuses on contrails. Bi-objective optimization is therefore a natural point of view. However, the aim is to minimize the global environmental impact, and for this we use a metric that is common in climate-change literature [15, 22, 23] to balance the two effects.

The amount of CO_2 emitted per liter of standard jet fuel is constant. A first assumption can thereby be made by equating the CO_2 emitted to the amount of fuel burned. As explained before, the problem is solved in 2D, and therefore no change in altitude is taken into account. In this case, for a given aircraft, the fuel flow, *i.e.*, the amount of fuel consumed per unit of flight time, is more or less constant. It will therefore be assumed hereafter that this fuel flow is constant, and that it is the same constant for all aircraft considered in the problem. This means that in order to minimize the CO_2 emitted, the overall flight time must be minimized. The assumption of an equal fuel flow for all aircraft can be challenged by simply applying a multiplicative factor to the flight time of some aircraft in the objective function, which is a straightforward adaptation of our optimization model.

Since the goal is to minimize the overall impact, it is necessary to quantify the impact of contrails versus that of CO_2 . For this, a metric known as *Global*

warming potential (GWP) is used. This metric relates the impact of most greenhouse gases to the impact of CO_2, under the form of a multiplicative factor considering that the impact of CO_2 corresponds to GWP = 1. This metric depends on a time horizon over which the impact is computed. More details about GWP can be found in [24]. Table 1 gives different values of GWP for contrails according to the different time horizons, H. In the sequel, *contrail-induced cirrus* (CIC) GWP will be noted g_H.

	$H = 20$ years	$H = 100$ Years	$H = 500$ years
$\mathrm{GWP}_{\mathrm{contrail}}(H)$	0.74	0.21	0.064
$\mathrm{GWP}_{\mathrm{CIC}}(H)$	2.2	0.63	0.19

Table 1: *Global warming potential* for contrail for various time horizons, H.

Depending on the time horizon considered, the contrails have more or less impact. Notably, they have less impact compared to CO_2 in the long term. In the following, only cirrus clouds induced by contrails will be taken into account, since there are the most impacting effect on the climate. However, contrails can also easily be considered, by a simple change in the cost function.

Without loss of generality, it will therefore be considered in the remainder of this paper that a unit of flight time in an area not favorable to contrails costs 1, and that a unit of flight time in an area favorable to persistent contrails costs $1 + g_H$, where H is the chosen time horizon (in years).

To summarize, the cost of arc (u, v) for aircraft i reads:

$$w_{u,v,i} = (1 + \lambda_{u,v} g_H) t_{u,v,i}, \tag{8}$$

where $\lambda_{u,v} \in [0, 1]$ is equal to the proportion of the arc (u, v) that lies is in a persistent contrail area, and $t_{u,v,i}$ is the time aircraft i spends flying one the arc (u, v). Remark that the flight time, $t_{u,v,i}$, depends upon the wind encountered. Both $\lambda_{u,v}$ and $t_{u,v,i}$ are input data.

The sliding-window approach mentioned before is adapted in the case of such weather-dependent cost functions, since there are uncertainties on weather forecast. In particular, contrails are difficult to predict, and their impact is even more difficult to predict [25]. Considering short-term path computation mitigates the uncertainties.

Details about how weather data are processed for the cost-function computation can be found in Appendix B.

3.4. Data

This subsection details the input data of the problem. It explains in particular how the graph is built, and how the sectors are defined. The wind encountered and the areas favorable to contrails are also known data but the process to obtain the related information is detailed in Appendix B.

The present study follows the new principle of *free route airspace* (FRA) which is applied nowadays to the European upper airspace. The aim of FRA is to remove the previously-established principle of air routes, and to replace it by navigation points, called waypoints, through which aircraft pass freely. A flight plan is therefore a simple sequence of waypoints through which the aircraft flies. This new paradigm allows one to consider an increased number of possible direct routes. As a consequence, the distance flown and thereby the CO_2 emissions, can be decreased.

Rules are still established to fly from a point to another even if there number aims to be decreased. Here, these rules are approximated by the rules established to build the graph $G = (V, A)$ required for the optimization model. The vertex set, V, consists of the waypoints. The arcs (set A) connect two waypoints when their inter distance is less than some user-defined threshold distance, $\overline{D}$. One could alternatively consider the complete graph, but this would not be coherent with operational practice, not to mention the increase of complexity in regards with the preliminary nature of the present study.

We construct our instances based on only the French waypoints that are located in the western and southern parts for now, see Figure 4 (the arcs are not displayed as they depend upon the maximum threshold distance, $\overline{D}$, chosen).

Our set of arcs is therefore:

$$A = \{(u, v) \mid u \in V, v \in V, d_{u,v} \leq \overline{D}\}, \tag{9}$$

where V is the set of waypoints, and $d_{u,v}$ is the distance between waypoints u and v.

For the subgraph capacities, the partition of the set A of arcs into N subsets, called sectors, $\{A_k\}_{k=1,2,\ldots,N}$, is initially defined with respect to waypoint set, as shown in Figure 5 for our instances. Then, all arcs with one of its ends in one such vertex sector is considered to be in this (arc) sector: $A_k = \{(u, v), u \in V_k \text{ or } v \in V_k\}$, where V_k is the subset of vertices that are in vertex sector k.

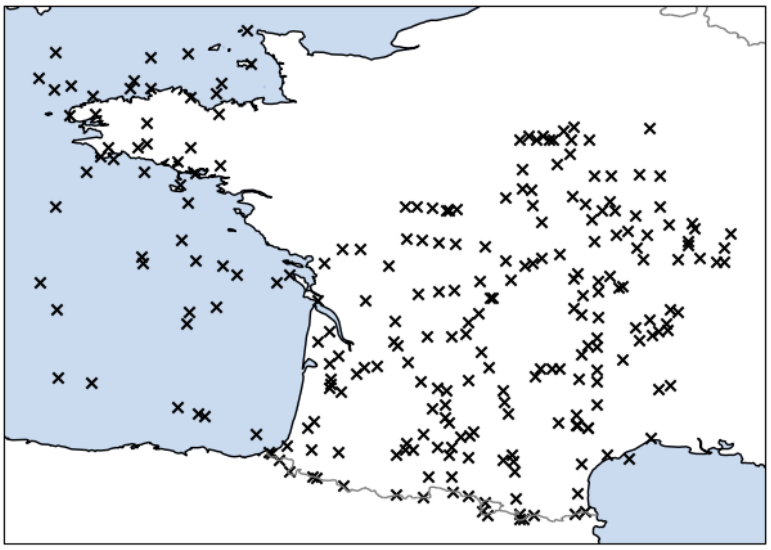

Figure 4: The FRA waypoints above France constituting our instance set.

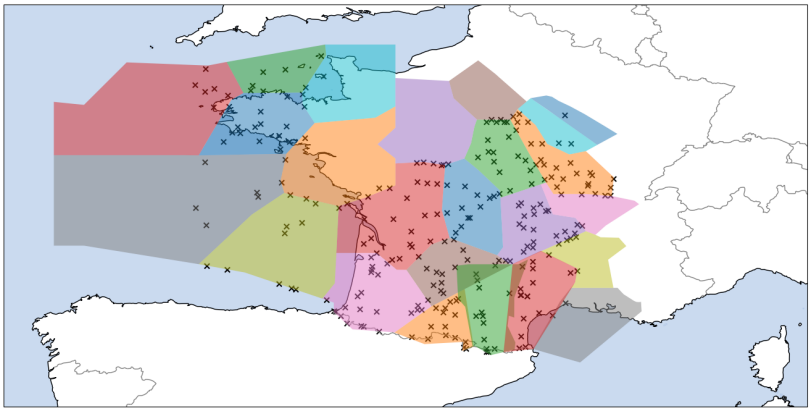

Figure 5: Vertex sectors considered above France for building the arc sectors for our instances.

The next section reports computational results.

4. Results and sensitivity analysis

This section presents an illustrative instance of the subgraph-capacity multiple shortest path problem together with various results obtained from numerical experiments resulting from a sensitivity analysis of the different parameters involved. An example of results is given in Subsection 4.1. Then, Subsection 4.2 focuses on the impact of wind on the results, while Subsection 4.3 addresses the impact of the time horizon chosen for the GWP computation on the results. Finally, the impact of the imposed airspace capacity, C_k, for sector $A_k,\ k = 1, 2, \ldots, N$, is discussed in Subsection 4.4.

4.1. Description of the illustrative instance

In the sequel, one instance of the problem is addressed but with various cost functions and various levels (right-hand side) for the capacity constraints. This subsection details the definition of this instance.

The graph is computed thanks to rules detailed in Section 3 (see Figures 4 and 5). Twenty aircraft are entering (taking off or entering the French upper airspace) per 30 minutes simultaneously for 3 hours. The source-end vertex pair (s_i, e_i) of each aircraft i, $i = 1, 2, \ldots, M$, are chosen randomly i, the vertex set so that the minimum distance (as the crow flies) is 200 Nautical Miles and the instance is then named FRA-200. A Nautical Mile (NM) is the distance unit used in aeronautics, and corresponds to 1.852 km. In order to define the arc set, A, we set the maximum distance between two linked points at $\overline{D} = 75$ NM. The airspeed of all aircraft is set to 400 knots (a knot (kt) is the speed unit used in aeronautics and corresponds to 1 NM/h or 1.852 km/h). This speed is chosen in adequacy with the typical airspeed of a standard commercial aircraft, namely the Airbus A320 [26]. Figure 6 displays the wind encountered, and Figure 7 shows the persistent contrails areas.

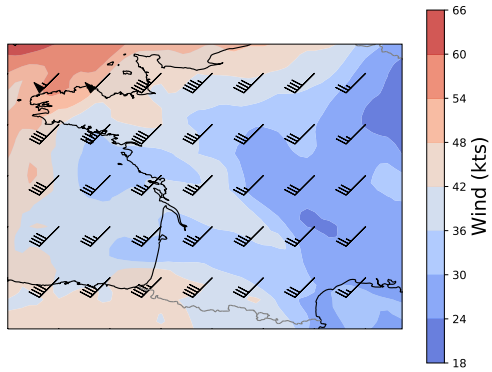

Figure 6: Wind encountered in instance FRA-200.

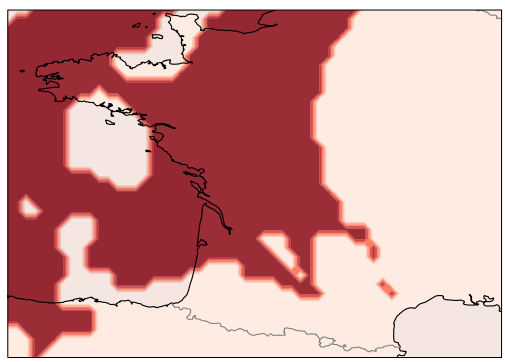

Figure 7: Persistent-contrail areas used for instance FRA-200.

The size of the sliding window for time-dependence consideration is set to $\Delta t = 15$ minutes. The parameter K for capacity consumption (as defined in Equation 7) is set to $K = 1.25$. If nothing else is explicitly mentioned, it is considered that:

- the capacity of each sector k is set to $C_k = 20,\ k = 1, 2, \ldots, N$;
- the time horizon chosen for the GWP computation is set to $H = 100$ years.

Table 2 summarizes the features for instance FRA-200. The details about the instance can be found in [27].

Feature	**Notation**	**FRA-200**
Aircraft and trajectory features		
Number of aircraft	M	20 per 30 minutes for 3 hours
Airspeed of aircraft		400 kts
Minimum distance between s_i and e_i		200 NM
Airspace features		
Number of sectors	N	23
Maximum distance for arc definition	$\overline{D}$	75 NM
Capacity of each sector	C_k	20
Optimization model features		
Time-window size	Δt	15 minutes
Time horizon for the GWP computation	H	100 years

Table 2: Features of the illustrative instance.

Instance FRA-200 is solved using the sliding window process explained in Subsection 2.2. The following results are obtained with the Java API of CPLEX on a computer with an Intel Core i5-10210U, 1.60 Hz, with 8 Go RAM and a Debian Linux OS. Figure 8 shows the solution obtained on instance FRA-200 on maps. The trajectories are represented by groups of 20 aircraft on different maps for reading purposes. The computation time is 137.2 s.

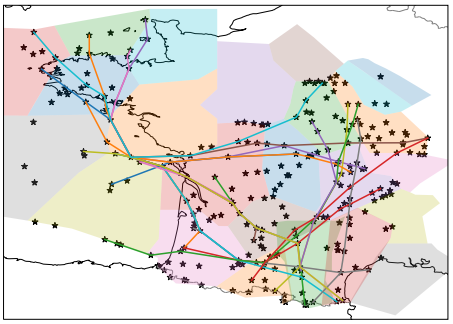

(a) Flights 0-19

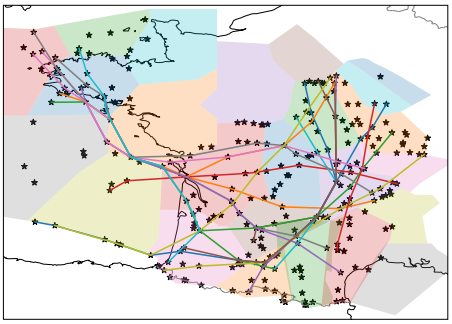

(b) Flights 20-39

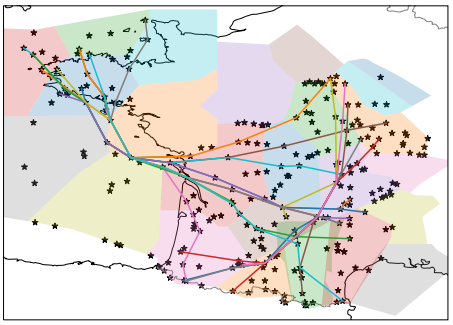

(c) Flights 40-59

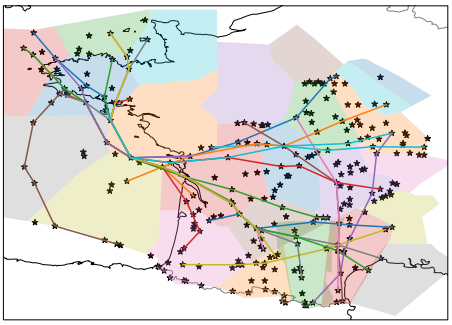

(d) Flights 60-79

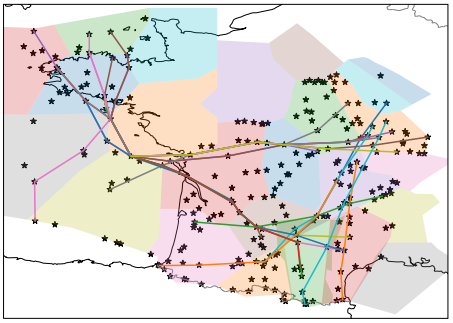

(e) Flights 80-99

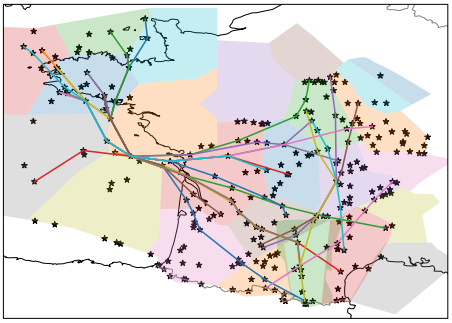

(f) Flights 100-119

Figure 8: Results obtained on instance FRA-200, grouped by 20 aircraft, sorted by increasing entry time.

In the sequel, the instance under study is instance FRA-200.

4.2. Impact of wind

The wind has a certain impact on the results. To quantify this impact, two variants of instance FRA-200 have been solved:

1. without wind and without contrails: $w_{u,v,i} = d_{u,v},\ (u,v) \in A,\ i = 1, 2, \ldots, M$;
2. with wind and without contrails: $w_{u,v,i} = t_{u,v},\ (u,v) \in A,\ i = 1, 2, \ldots, M$.

Figure 9 displays the additional flight distance and flight time in the second case (with wind) in comparison to the first case (without wind).

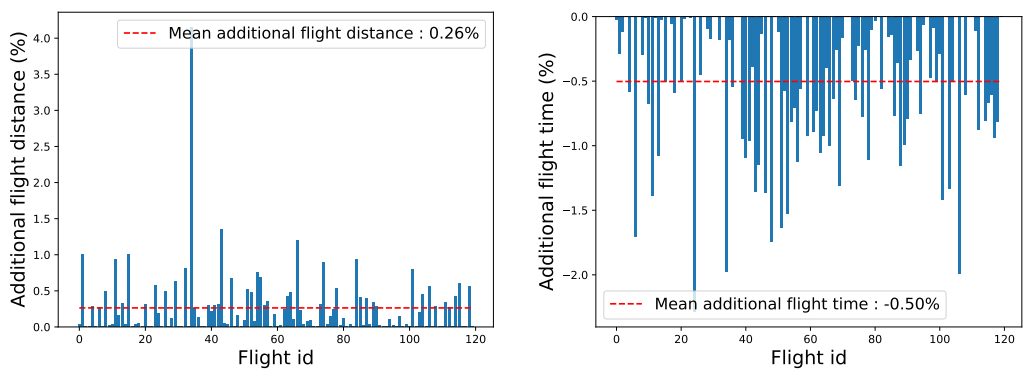

(a) Additional flight distance

(b) Additional flight time

Figure 9: Additional flight time and flight distance when wind is considered (flight time minimization) in comparison with results obtained when wind is not taken into account (only distance is minimized: $w_{u,v,i} = d_{u,v}$).

The results show that in general, the flight distance is increased to the benefit of a reduced flight time, which was expected.

4.3. Impact of the time horizon used for GWP computation

As explained in Subsection 3.3, the cost factor associated with contrails depends on the chosen time horizon, H. Intuitively, the shorter the time horizon, the more impact the contrails have, and therefore the more beneficial it is to lengthen the trajectories to avoid contrails. To confirm this thought, three variants of instance FRA-200 are solved:

1. no contrail consideration: $g_H = 0$;
2. contrails consideration with $H = 100$ years: $g_H = g_{100} = 0.63$;
3. contrails consideration with $H = 20$ years: $g_H = g_{20} = 2.2$.

Figures 10 and 11 display comparative results for variants 1 and 2, and for variants 1 and 3, respectively.

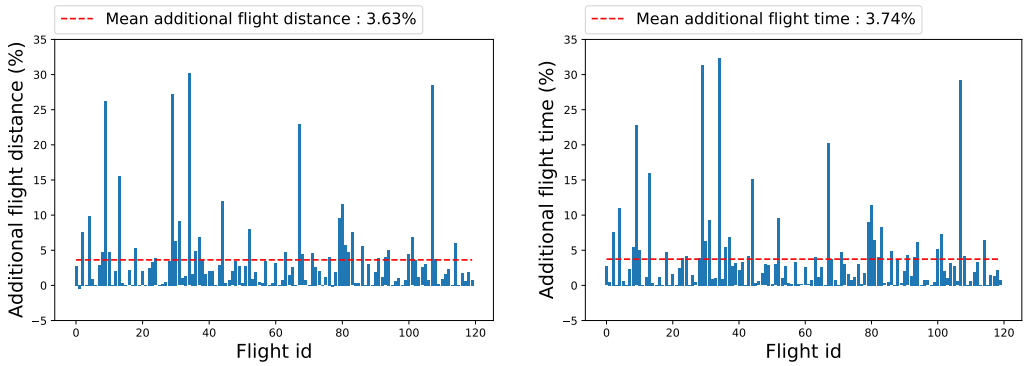

(a) Additional flight distance

(b) Additional flight time

Figure 10: Additional flight time and flight distance when $H = 100$ years ($g_H = g_{100} = 0.63$) when compared with the case without contrails ($g_H = 0$).

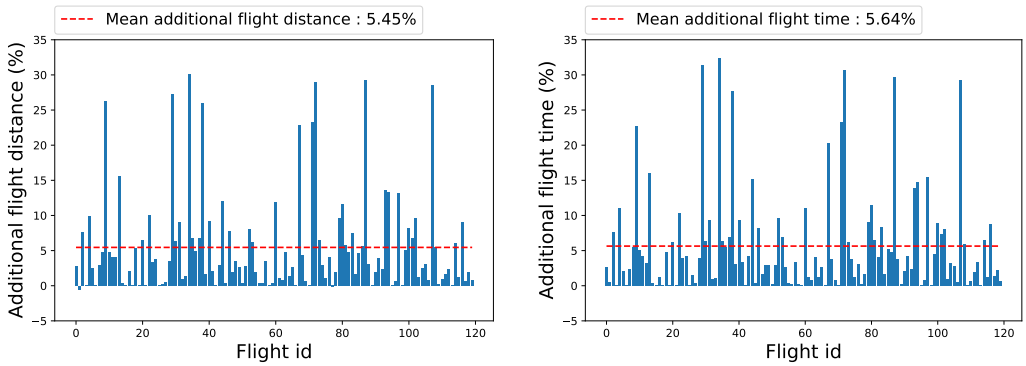

(a) Additional flight distance

(b) Additional flight time

Figure 11: Additional flight time and flight distance when $H = 20$ years ($g_H = g_{20} = 2.2$) when compared with the case without contrails ($g_H = 0$).

The flight time is higher because of the avoidance of contrail area. Figures 10 and 11 show that the dependence on the time horizon is important since in the case of a short horizon the optimal trajectories are much longer than in the case of a longer time horizon. If the contrails impact is considered high, the flight time has a lower impact on the objective-function, and then is

highly increased to avoid as much as possible the areas favorable to contrails. Indeed, Figure 11 shows optimal trajectories with an increase of more than 30% in flight time. Fuel consumption therefore explodes from an environmental point of view, it is not necessarily relevant to choose such a trajectory. It is also economically costly (increase in fuel and extra cost associated to flight delays). Finally, such extra consumption has also an impact on safety since a significant part of the extra fuel that every aircraft must carry in order to anticipate a possible diversion to another airport will be used for avoiding contrails. An extra constraint should therefore be added to our optimization model to avoid such undesirable solutions. Such an extra constraint is also likely to satisfy other operational needs. For example, if an airline is planning connections between its flights, it is desirable that the flights involved are not delayed too much so that the connection is guaranteed.

Let $t_{0,i}$ be the flight time without any contrail consideration. It can be computed thanks to the optimization process with $g_H = 0$. We propose to add to the model constraints $\sum_{(u,v)\in A} t_{u,v,i}\ x_{u,v,i} \leq C\ t_{0,i},\ i = 1, 2, \ldots, M$, where $t_{u,v,i}$ is the flight time over the arc (u, v) for the flight i, and where C is a user-defined constant to control the additional flight time allowed.

Figure 12 shows an example of results obtained when such constraints are added with $C = 1.1$, (10% of additional flight time is allowed).

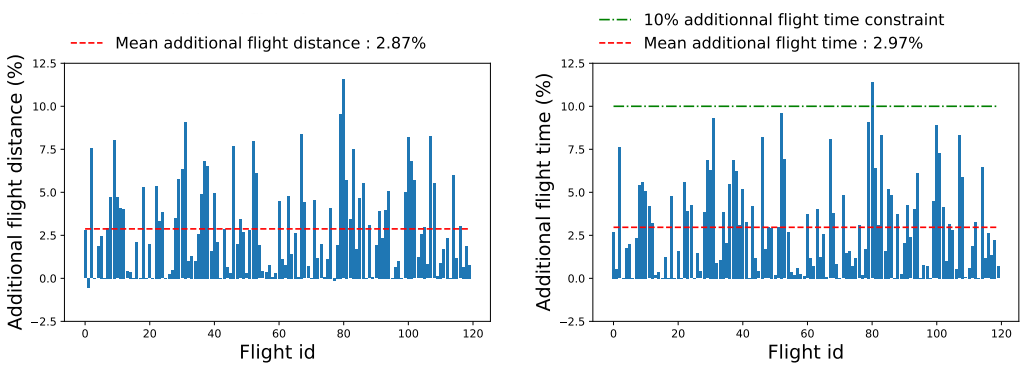

(a) Additional flight distance

(b) Additional flight time

Figure 12: Additional flight time and flight distance with extra flight time constraints added when $H = 20$ years, in comparison with the case without contrails.

Because of the sliding-window process, the extra constraints are not globally respected, but they are respected locally at each step, and are nearly

respected at the global scale, as can be observed in Figure 12.

4.4. Impact of airspace capacity

A last parameter to be studied is airspace capacity. The same setup concerning aircraft is taken with a GWP computed with, this time, $H = 100$ years. Several results are impacted by changing the airspace capacity C_k, $k = 1, 2, \ldots, N$, especially the obtained optimal objective-function value, and the computation time. Indeed, in order to satisfy capacity constraints, some aircraft may be forced to fly longer or through contrail zones. The problem can be harder to solve if the capacity constraints are restrictive, and so the computation time increases. Figure 13 shows the evolution of the optimal objective-function value and the computation time obtained for various capacity levels, C_k, assumed constant for every sector k, $k = 1, 2, \ldots, N$, and at each time window.

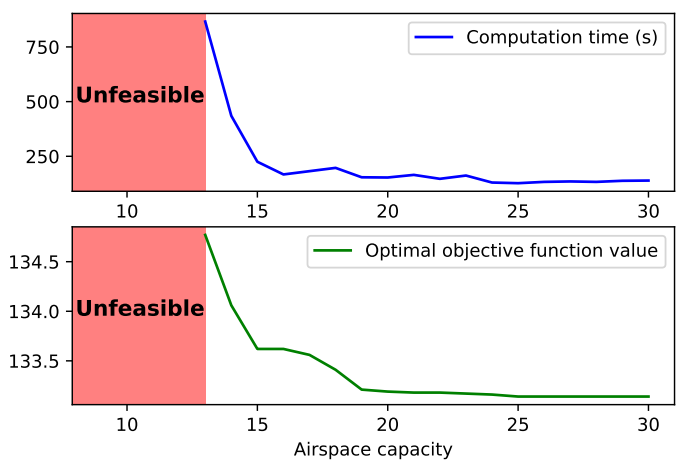

Figure 13: Results comparison in terms of objective-function value and computation time when the airspace capacity, C_k, changes.

The above results show how the right-hand side of the airspace capacity constraints affect the feasibility of the problem and the environmental impact. The higher the capacity of the airspace is, the better the results are. However, beyond a certain value of C_k, no change is observed in computation time, nor in objective-function value since the capacity constraints are not saturated.

5. Conclusion

We introduced a new model for the multiple shortest-path problem that takes into account capacity constraints on subgraphs. In the static case, the model is based on the computation of the number of vehicles occupying each subgraph. Dynamic aspects have also been taken into account by establishing an adapted model with time windows over each of which the static model is solved. Taking this time-dependent aspect into account is essential because as vehicles move, they free up capacity and costs can also change over time. The model used does not provide the same quality of solution as if the static model had been discretized in time, but it fits better the operational reality as illustrated by the application addressed in our study. Moreover, it was shown that the problem could be solved directly by a standard commercial solver without deploying special techniques.

The application addressed in this paper gives a new model for the contrail-avoidance problem when considered at the network scale and from the air traffic control point of view. A time-window strategy has been chosen in this study to model the time-dependence because the time during two contrail predictions can be high. Work has also been done on the cost of arcs, so that they can be adapted to the ATM point of view. This allows one to consider other non-CO_2 effects due to air transport, or to use more elaborate metrics to determine the impact of contrails.

Future tracks of research should focus on the numerous sources of uncertainty to be taken into account when addressing the contrail-avoidance problem. There are several uncertainties to consider when studying contrail-favorable (or persistent-contrail-favorable) areas, as shown by Gierens *et al.* [25]. Other source of uncertainty are the wind estimation and the presence of traffic.

Moreover, when considering the air traffic control point of view, one faces another crucial criterion: fairness. It was not explicitly optimized in this preliminary study. Future work should adapt the proposed model so as to quantify and enforce equity between airlines.

Finally, the cruise altitude should also be envisaged as decision variables since it is an efficient mean of mitigating contrail impact, as shown by Fichter *et al.*[28].

This leads to several issues including the knowledge of some critical aircraft parameters (such as its mass at any moment) which are not always known from the air traffic control point of view. Moreover, fuel consumption

depends on the altitude as well as on the type of aircraft. It could thereby be considered to use models allowing to have the same information as those of the air traffic control while approaching the true fuel flows. For that, the OpenAP [29] database could be used, or other models based on machine learning as it has been done in [30] for the approach and landing phases.

Appendix A. Time discretized optimization model

The mathematical optimization model obtained in the static case can be discretized to obtain the time-dependent optimization model. This transformation is based on the classical *time-dependent shortest path* problem [31].

Some notations should be defined first:

- $T_i = \{t_{0,i}, \ldots, t_{f,i}\}$: the set of time periods for vehicle i;
- $T = \bigcup_{i=1}^{M} T_i$;
- $C_{k,t}$: the capacity of sector k, $k = 1, \ldots, N$, during time period t, $t \in T$;
- $w^t_{u,v,i}$: the cost for vehicle i, $i = 1, \ldots, M$, to go through arc $(u, v) \in A$ at time period t, $t \in T_i$;
- $\Delta^t_{u,v,i}$: the time necessary for vehicle i, $i = 1, \ldots, M$, to go through arc $(u, v) \in A$ at time period t, $t \in T_i$.

The decision variables are:

- $x_{u,v,i} \in \{0, 1\}$ is equal to 1 if vehicle i goes through arc (u, v);
- $z^t_{u,v,i} \in \{0, 1\}$ is equal to 1 if vehicle i enters arc (u, v) at time period t;
- $y^t_{k,i} \in \{0, 1\}$ is equal to 1 if vehicle i flies through sector k at time period t, $t \in T$.

The model is then:

$$\min_{X,Y,Z} \quad \sum_{i=1}^{M} \sum_{t \in T_i} \sum_{(u,v) \in A} w^t_{u,v,i} z^t_{u,v,i} \tag{A.1a}$$

$$\text{s.t.} \quad \sum_{(u,v) \in A} x_{u,v,i} - \sum_{(v,u) \in A} x_{v,u,i} = 0,\ u \in V \backslash \{s_i, e_i\},\ i = 1, 2, \ldots, M \tag{A.1b}$$

$$\sum_{(s_i,v) \in A} x_{s_i,v,i} - \sum_{(v,s_i) \in A} x_{v,s_i,i} = 1,\ i = 1, 2, \ldots, M \tag{A.1c}$$

$$\sum_{(e_i,v) \in A} x_{e_i,v,i} - \sum_{(v,e_i) \in A} x_{v,e_i,i} = -1,\ i = 1, 2, \ldots, M \tag{A.1d}$$

$$\sum_{(u,v) \in A} z^t_{u,v,i} - \sum_{(v,u) \in A} z^{t+\Delta^t_{v,u,i}}_{v,u,i} = 0,\ u \in V \backslash \{s_i, e_i\},\ i = 1, 2, \ldots, M,\ t \in T_i \tag{A.1e}$$

$$\sum_{(s_i,v) \in A} z^{t_{0,i}}_{s_i,v,i} = 1,\ i = 1, 2, \ldots, M \tag{A.1f}$$

$$\sum_{t \in T_i} z^t_{u,v,i} = x_{u,v,i},\ (u,v) \in A,\ k = 1, \ldots, N,\ i = 1, \ldots, M \tag{A.1g}$$

$$\sum_{i=1}^{M} y^t_{k,i} \leq C_{k,t},\ k = 1, 2, \ldots, N,\ t \in T \tag{A.1h}$$

$$y^t_{k,i} = 1 \text{ iff } \sum_{(u,v) \in A_k} z^t_{u,v,i} \geq 1,\ i = 1, 2, \ldots, M,\ k = 1, 2, \ldots, N,\ t \in T_i \tag{A.1i}$$

$$y^t_{k,i} = 0,\ i = 1, 2, \ldots, M,\ k = 1, 2, \ldots, N,\ t \in T \backslash T_i \tag{A.1j}$$

$$X_i \in \{0,1\}^{|A|},\ i = 1, 2, \ldots, M \tag{A.1k}$$

$$Z_{i,t} \in \{0,1\}^{|A|},\ i = 1, 2, \ldots, M,\ t \in T_i \tag{A.1l}$$

$$Y_{i,t} \in \{0,1\}^{N},\ i = 1, 2, \ldots, M,\ t \in T_i \tag{A.1m}$$

Constraints (A.1b),(A.1c) and (A.1d) are the flow conservation constraints. Constraints (A.1e) and (A.1f) enforce consistency of space-time flow conser-

vation. Constraints (A.1g) make the link between the time-dependent and the static decision variables. Constraints (A.1h) are the time-discretized capacity constraints. Constraints (A.1i) and (A.1j) define the auxiliary variables $y^t_{k,i}$. The former can easily be linearized, as for the static model (see Proposition 1).

Appendix B. Data processing for numerical experiments

This section shows how data for computational experiments have been extracted and computed. Appendix B.1 deals with wind data, while Appendix B.2 focuses on contrail data.

Appendix B.1. Wind data

The costs defined by (8) involves the computation of the flight time over each arc $(u, v) \in A$. For this, the wind on the arcs, and the distance between u and v, the two ends of the arcs, have to be known.

Let λ_u and λ_v be the latitude of vertices u and v respectively, and let ϕ_u and ϕ_v be their longitude. The distance between u and v is given by:

$$d_{u,v} = R\ c_{rad}(km), \tag{B.1}$$

$$= 60\ c_{degrees}(NM), \tag{B.2}$$

where $R = 6,371$ km is the Earth radius, c_{rad} and $c_{degrees}$ represent the following c values, expressed in radians and in degrees respectively:

$$c = \arccos\Big(\sin(\lambda_u)\ \sin(\lambda_v) + \cos(\lambda_u)\ \cos(\lambda_v)\ \cos(\phi_v - \phi_u)\Big). \tag{B.3}$$

Then, the flight time for aircraft i, noted $t_{u,v,i}$, between points u and v is given by:

$$t_{u,v,i} = \frac{d_{u,v}}{GS_{u,v,i}}, \tag{B.4}$$

where $GS_{u,v,i}$ is the ground speed of aircraft i on arc (u, v). It can be computed via:

$$GS_{u,v,i} = V_{a_i} + W_{u,v}, \tag{B.5}$$

where V_{a_i} is the airspeed of aircraft i (considered constant), and $W_{u,v}$ is the wind encountered on the arc (u, v).

Wind data have been extracted from the website Windy [32] on a square grid of size 0.2 degree above France, as shown on Figure B.14.

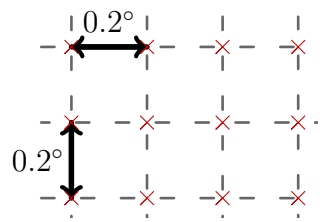

Figure B.14: 2D grid used for wind data extraction from Windy [32].

To compute the wind on each node of the graph, a so-called Shepard interpolation [33] was used. More precisely, for each node P located in a 2D-square $P_1P_2P_3P_4$ of the data grid, the wind $W(P)$ at P is calculated from the wind at $P_k,\ k = 1, 2, 3, 4$, using the distance from P to each of these points (noted respectively d_1, d_2, d_3 and d_4) as follows:

$$W(P) = \frac{\sum_{i=1}^{4} W(P_i) * d_i^{-p}}{\sum_{i=1}^{4} d_i^{-p}}, \tag{B.6}$$

where $p > 1$ is a user-defined parameter (set to $p = 2$ in this study). Figure B.15 summarizes the notations required to compute the wind at P from the known winds at $P_k,\ k = 1, 2, 3, 4$.

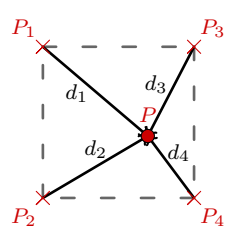

Figure B.15: Notations for estimating the wind at P via Shepard interpolation.

Finally, the wind along an arc (u, v) is simply defined as the average of that at u and at v:

$$W_{(u,v)} = \frac{W(u) + W(v)}{2}. \tag{B.7}$$

Figure B.16 shows data used for the examples presented in the result section (Section 4).

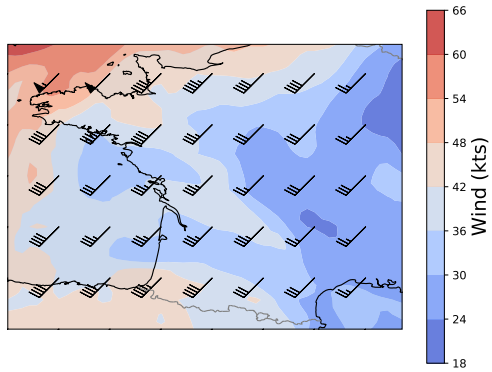

Figure B.16: Wind encountered in the example of the result.

Appendix B.2. Contrail data

Contrails are formed in cold and humid areas. They persist and induce cirrus if the air is supersaturated in ice. The computation of persistent contrail areas is performed in two phases:

1. Areas favorable to contrail formation
2. Areas in which contrails will persist (ice supersaturated areas).

In [23], contrails areas are computed thanks to the *Schmidt-Appleman criterion*. This criterion gives a minimum threshold, r_{min}, of relative humidity of the air in liquid water, noted RH_w, above which contrails are formed: contrails are assumed to form when $RH_w \geq r_{min}$, where

$$r_{min} = \frac{G(T - T_c) + e_{sat}^{liq}(T_c)}{e_{sat}^{liq}(T)}, \tag{B.8}$$

$e_{sat}^{liq}(T)$ is the saturation vapor pressure over water, T_c is the estimated threshold temperature (in Celsius degrees) for contrail formation at liquid saturation. The later is computed via:

$$T_c = -46.46 + 9.43 \log(G - 0.053) + 0.72 \log^2(G - 0.053), \tag{B.9}$$

where $G = \frac{EI_{H_2O}C_pP}{\epsilon Q(1-\eta)}$, $EI_{H_2O} = 1.25$ is the water vapor emission index, $C_p = 1004\ J.kg^{-1}.K^{-1}$ is the heat capacity of the air, P is the ambient pressure (in Pascals), $\epsilon = 0.6222$ is the ratio of the molecular masses of water and dry air, $Q = 43 * 10^6 J.kg^{-1}$ is the specific heat of combustion, and $\eta = 0.3$ is the average propulsion efficiency of a commercial aircraft.

In [23], the ice super saturated areas are determined thanks to the following criterion: $RH_i > 1$, where the relative humidity over the ice, noted RH_i is computed as follows:

$$RH_i = RH_w * \frac{6.0612 * \exp(\frac{18.102*T}{249.52+T})}{6.1162 * \exp(\frac{22.577*T}{273.78+T})}, \tag{B.10}$$

and where T is the ambient temperature in Celsius degrees.

The relative humidity and temperature are also computed from data extracted from Windy [32] on a 2D-grid, and interpolated via quadratic interpolation. Figure B.17 shows the data used for the examples presented in the result section (Section 4), where red areas are persistent-contrail-favorable areas to be avoided.

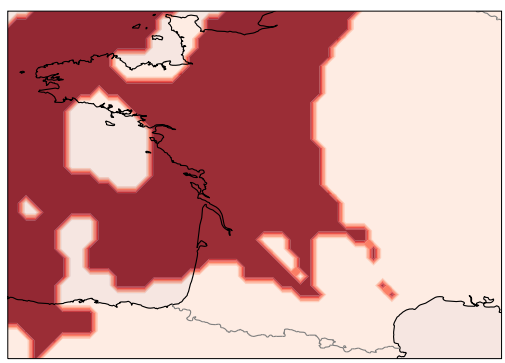

Figure B.17: Persistent-contrail areas used for our instances.

Acknowledgements

The authors thank DGAC (French civil aviation authority) for prompting and funding this work, and more specifically its DTA and DSNA services. Their inputs and expertise were also essential to the achievement of this work.

References

[1] C. H. Papadimitriou, K. Steiglitz, Combinatorial optimization: Algorithms and complexity, Courier Corporation, 1998.

[2] E. W. Dijkstra, A note on two problems in connexion with graphs, Numerische Mathematik 1 (1959) 269–271.

[3] D. Lee, D. Fahey, A. Skowron, M. Allen, U. Burkhardt, Q. Chen, S. Doherty, S. Freeman, P. Forster, J. Fuglestvedt, A. Gettelman, R. De León, L. Lim, M. Lund, R. Millar, B. Owen, J. Penner, G. Pitari, M. Prather, R. Sausen, L. Wilcox, The contribution of global aviation to anthropogenic climate forcing for 2000 to 2018, Atmospheric Environment 244 (2021) 117834.

[4] R. Bellman, On a routing problem, Quarterly of Applied Mathematics 16 (1958) 87–90.

[5] D. G. Luenberger, Introduction to dynamic systems: Theory, models, and applications, Wiley, New York, 1979.

[6] L. Lozano, A. L. Medaglia, On an exact method for the constrained shortest path problem, Computers & Operations Research 40 (2013) 378–384.

[7] L. D. P. Pugliese, F. Guerriero, A survey of resource constrained shortest path problems: Exact solution approaches, Networks 62 (2013) 183–200.

[8] L. Santos, J. Coutinho-Rodrigues, J. R. Current, An improved solution algorithm for the constrained shortest path problem, Transportation Research Part B: Methodological 41 (2007) 756–771.

[9] J. G. Wardrop, J. I. Whitehead, Correspondance. Some theorical aspects of road traffic research, Proceedings of the Institution of Civil Engineers 1 (1952) 767–768.

[10] J. G. Wardrop, Road paper. Some theorical aspects of road traffic research, Proceedings of the Institution of Civil Engineers 1 (1952) 325–362.

[11] D. Bertsimas, S. S. Patterson, The air traffic flow management problem with enroute capacities, Operations Research 46 (1998) 406–422.

[12] A. Agustin, A. Alonso-Ayuso, L. Escudero, C. Pizarro, On air traffic flow management with rerouting. Part I: Deterministic case, European Journal of Operational Research 219 (2012) 156–166.

[13] L. Liberti, Reformulation techniques in mathematical programming, Thèse d'Habilitation à Diriger des Recherches (HDR), Université Paris IX, France (2007).

[14] L. Foschini, J. Hershberger, S. Suri, On the complexity of time-dependent shortest paths, in: Proceedings of the twenty-second annual ACM-SIAM symposium on Discrete algorithms, SIAM, 2011, pp. 327–341.

[15] B. Sridhar, H. K. Ng, N. Y. Chen, Aircraft trajectory optimization and contrails avoidance in the presence of winds, Journal of Guidance, Control, and Dynamics 34 (2011) 1577–1584.

[16] S. Hartjes, T. Hendriks, D. Visser, Contrail mitigation through 3D aircraft trajectory optimization, in: 16th AIAA Aviation Technology, Integration, and Operations Conference, American Institute of Aeronautics and Astronautics, Washington, D.C., 2016.

[17] S. Matthes, V. Grewe, K. Dahlmann, C. Frömming, E. Irvine, L. Lim, F. Linke, B. Lührs, B. Owen, K. Shine, S. Stromatas, H. Yamashita, F. Yin, A concept for multi-criteria environmental assessment of aircraft trajectories, Aerospace 4 (2017) 42.

[18] F. Yin, V. Grewe, C. Frömming, H. Yamashita, Impact on flight trajectory characteristics when avoiding the formation of persistent contrails for transatlantic flights, Transportation Research Part D: Transport and Environment 65 (2018) 466–484.

[19] J. Rosenow, H. Fricke, Impact of multi-criteria optimized trajectories on European airline efficiency, safety and airspace demand, Journal of Air Transport Management 78 (2019) 133–143.

[20] S. Campbell, N. Neogi, M. Bragg, An operational strategy for persistent contrail mitigation, in: 9th AIAA Aviation Technology, Integration, and Operations Conference (ATIO), American Institute of Aeronautics and Astronautics, Hilton Head, South Carolina, 2009.

[21] S. Campbell, N. Neogi, M. Bragg, An optimal strategy for persistent contrail avoidance, in: AIAA Guidance, Navigation and Control Conference and Exhibit, American Institute of Aeronautics and Astronautics, Honolulu, Hawaii, 2008.

[22] A. Simorgh, M. Soler, D. González-Arribas, S. Matthes, V. Grewe, S. Dietmüller, S. Baumann, H. Yamashita, F. Yin, F. Castino, F. Linke, B. Lührs, M. M. Meuser, A comprehensive survey on climate optimal aircraft trajectory planning, Aerospace 9 (2022) 146.

[23] M. Soler, B. Zou, M. Hansen, Flight trajectory design in the presence of contrails: Application of a multiphase mixed-integer optimal control approach, Transportation Research Part C: Emerging Technologies 48 (2014) 172–194.

[24] J. Fuglestvedt, K. Shine, T. Berntsen, J. Cook, D. Lee, A. Stenke, R. Skeie, G. Velders, I. Waitz, Transport impacts on atmosphere and climate: Metrics, Atmospheric Environment 44 (2010) 4648–4677.

[25] K. Gierens, S. Matthes, S. Rohs, How well can persistent contrails be predicted?, Aerospace 7 (2020) 169.

[26] Airbus A-320 | SKYbrary aviation safety, 2022. URL: `https://www.skybrary.aero/aircraft/a320`.

[27] C. Demouge, FRA-200 instance for subgraph-capacity multiple shortest path application to contrail avoidance, 2022. URL: `https://cloud.recherche.enac.fr/index.php/s/i6jxDFM8GnSAgyF`.

[28] C. Fichter, S. Marquart, R. Sausen, D. S. Lee, The impact of cruise altitude on contrails and related radiative forcing, Meteorologische Zeitschrift 14 (2005) 563–572.

[29] J. Sun, J. M. Hoekstra, J. Ellerbroek, OpenAP: An open-source aircraft performance model for air transportation studies and simulations, Aerospace 7 (2020) 104.

[30] G. Jarry, D. Delahaye, E. Féron, Approach and landing aircraft onboard parameters estimation with LSTM networks, in: AIDA-AT 2020, 1st conference on Artificial Intelligence and Data Analytics in Air Transportation, 2020.

[31] L. Yang, X. Zhou, Constraint reformulation and a Lagrangian relaxation-based solution algorithm for a least expected time path problem, Transportation Research Part B: Methodological 59 (2014) 22–44.

[32] Windyty SE, Windy API, 2022. URL: https://api.windy.com/.

[33] D. Shepard, A two-dimensional interpolation function for irregularly-spaced data, in: Proceedings of the 23rd ACM national conference, ACM Press, 1968, pp. 517–524.